A Narrowband Model For Aeronautical Telemetry Channels

Kenneth Welling
Department of Electrical & Computer Engineering
Brigham Young University
Provo, UT 84602
wellingk@.ee.byu.edu

Faculty Advisor:
Dr. Michael Rice

ABSTRACT

This paper presents a narrowband channel model appropriate for modeling multipath interference in aeronautical telemetry applications. This model uses a simplified version of Bello's aeronautical fading channel model [1] with the following three parameters: the specular to direct power ratio Γ, the direct to diffuse power ratio κ and the relative Doppler shift of the specular component. Data taken from Patuxent River NAWC, Edwards AFB and White Sands Missile Range demonstrate that the model is a reasonably accurate statistical representation of the envelope (and power) fluctuations observed in the data. The model works well for those cases where a dominate line-of-sight signal component exists, as well as for those cases where the power in the specular reflections is on the order of the power in the line-of-sight component.

INTRODUCTION

Multipath interference causes power fluctuations and signal dropouts or fades in aeronautical telemetry [9], [3]. Error control coding can increase reliability, but first the signal fading characteristics of the channel need to be understood. The aeronautical telemetry channel can be represented using a simplified version of the three component model proposed by Bello [1]. Using the Bello model the received signal $y(t)$ is represented by

$$\begin{aligned} y(t) &= As_0(t) + Bs_0(t-\tau_{\mathrm{sp}})\exp\{j\Delta\omega_{\mathrm{sp}}(t-\tau_{\mathrm{sp}})\} + \sum_k a_k s_0(t-\tau_k)\exp\{j\Delta\omega_k(t-\tau_k)\} && (1) \\ &= \underbrace{As_0(t)}_{\text{line-of-sight component}} + \underbrace{Bs_0(t-\tau_{\mathrm{sp}})\exp\{j\Delta\omega_{\mathrm{sp}}(t-\tau_{\mathrm{sp}})\}}_{\text{specular reflection component}} + \underbrace{\xi(t)\exp\{j\Delta\omega_{\mathrm{diff}}(t-\tau_{\mathrm{diff}})\}}_{\text{diffuse multipath component}} && (2) \end{aligned}$$

where $s_0(t) = \exp\{j\pi h b_n t/T_b\}$ is the complex baseband representation of the PCM/FM signal (h is the modulation index which is usually set to 0.7 times the bit time, $b_n \in \{-1,+1\}$ is the information bit, and T_b is the bit time). The line-of-sight component is a result of the direct line-of-sight propagation (with amplitude A) between the transmitter and the receiver. The specular reflection component models the attenuated and delayed version of the line-of-sight component that often occurs due to reflection (from the ground, mountain, sea surface, or wing) or the path difference between the feeds to two transmit antennas on the airborne platform. This component has magnitude B, average time delay τ_{sp} and average Doppler shift $\Delta\omega_{sp}$. The diffuse component consists of all other low level multipath reflections which is modeled as a single random component $\xi(t)$ with average delay τ_{diff} and average Doppler shift $\Delta\omega_{\mathrm{diff}}$. Bello models this component as a complex zero mean Gaussian random process with variance σ_d^2. This expression has been normalized so that the direct component has no time or frequency shift. This normalization is appropriate if a frequency tracker is used at the receiver to track the carrier frequency of the direct component and if only the relative time delay between the direct ray and the specular and diffuse components is of interest.

Nelson [7] identified Bello's model to be appropriate for describing fading on aeronautical telemetry channels at military test ranges, and evaluated the performance of PCM/FM over this channel as a function of

$$\Gamma = \frac{B^2}{A^2} \qquad \frac{\text{specular reflection power}}{\text{line-of-sight component power}} \tag{3}$$

$$\kappa = \frac{A^2}{2\sigma_d^2} \qquad \frac{\text{line-of-sight component power}}{\text{diffuse component power}}, \tag{4}$$

and the relative Doppler shift of the specular component. These parameters can be determined from an accurate statistical model. This paper discusses fade statistics, parameter estimation, and results and conclusions.

FADE STATISTICS

Envelope data derived from AGC and AM signals measured at Edwards Air Force Base, White Sands Missile Range and Patuxent River NAWC were used to test how well the Bello model represents the fading statistics of real aeronautical telemetry channels. The data collection and signal processing are described in Appendix A.

Fade predictions can be made from the cumulative distribution of the envelope variations. The probability density function and cumulative distribution of the received PCM/FM envelope using the Bello channel model are a function of Γ, κ , and the Doppler shifts. The only available channel sounding data are the AGC and AM signals from which the signal envelope can be reconstructed. Since envelope data provides no information on the phase and delay, these parameters are grouped into a phase term which is assumed uniformly distributed on $[-\pi,\pi]$ thereby producing a simplified version of Bello's model which is a function only of Γ and κ (or equivalently, of A, B, and σ_d^2). These parameters are estimated from histograms of the received envelope derived from AGC and AM data by finding the values of A, B, and σ_d^2 which make the theoretic probability density function and the histogram match the best.

The envelope of $y(t)$ is given by

$$e(t) = \sqrt{[A + B\cos\theta(t) + N_c(t)]^2 + [B\sin\theta(t) + N_s(t)]^2} \tag{5}$$

where $N_c(t)$ and $N_s(t)$ are the real and imaginary (i.e. quadrature) components of $\xi(t)$ and

$$\theta(t) = \Delta\omega t + \left(\frac{\pi h b_n}{T_b} + \Delta\omega\right)\tau_{\mathrm{sp}} \tag{6}$$

is the phase shift between the line-of-sight component and the specular reflection. At any time instant t', the envelope $y(t') = R$ is a Rice random variable with probability density funcion

$$p_{\mathrm{R}}(r) = \frac{r}{\sigma_d^2}\exp\left\{-\frac{r^2 + A^2 + B^2 + 2AB\cos\theta(t')}{2\sigma_d^2}\right\} I_0\left(\frac{r\sqrt{A^2 + B^2 + 2AB\cos\theta(t')}}{\sigma_d^2}\right). \tag{7}$$

Since the envelope data available provide no phase information, the phase $\theta(t')$ is assumed uniformly distributed on $[-\pi,\pi]$ and the density function (7) is treated as a conditional density function $P_{\mathrm{R}}(r|\theta(t'))$. The total probability theorem [8] is used to derive the envelope probability density function which depends only on A, $\mathbf{B}$, and σ_d^2:

$$p_{\mathrm{R}}(r) = \int_\theta p(r|\theta)p(\theta)d\theta \tag{8}$$

$$= \frac{r}{2\pi\sigma_d^2}\int_{-\pi}^{\pi} e^{-\frac{r^2+A^2+B^2+2AB\cos(\theta)}{2\sigma_d^2}} I_0\left(\frac{r\sqrt{A^2+B^2+2AB\cos(\theta)}}{\sigma_d^2}\right) d\theta \tag{9}$$

where $\theta = \theta(t')$.

PARAMETER ESTIMATION

To find the best values of A, B, and σ_d^2 to model the data measured at test ranges, a histogram of the envelope of each run is produced and compared with the theoretic probability density function (9) for a given set of parameters A, B, and σ_d^2. The set of parameters for which (9) and the histogram most closely match are the parameters we use to model the channel for that run.

The data histogram is created by partitioning the envelope voltages samples v_i, i = 1,2...n into into N bins of equal width V_{max}/N, ranging from 0 to V_{max} according to

$$\begin{array}{ll} P_1 & \left[0, \frac{V_{max}}{N}\right) \\ P_2 & \left[\frac{V_{max}}{N}, \frac{2V_{max}}{N}\right) \\ P_3 & \left[\frac{2V_{max}}{N}, \frac{3V_{max}}{N}\right) \\ \vdots & \vdots \\ P_k & \left[\frac{(k-1)V_{max}}{N}, \frac{kV_{max}}{N}\right) \\ \vdots & \vdots \\ P_N & \left[\frac{(N-1)V_{max}}{N}, V_{max}\right]. \end{array} \tag{10, 11}$$

The value for each bin of the histogram is determined by the relative frequency that samples fall into the respective bin range, determined by

$$h_k = \frac{n_k}{n} \tag{12}$$

where n is the total number of samples, and n_k is the number of samples that fall within the range P_k of a given bin, according to

$$n_k = \left|\left\{ i \left| \frac{(k-1)V_{max}}{N} \le v_i \le \frac{kV_{max}}{N} \right.\right\}\right|. \tag{13}$$

Let $P_R\,(r; A, B, \sigma_d^2)$ be the theoretical density function given by (9). Closeness of fit is measured by the squared error which is the square of the difference between h_k and the area under $P_R\,(r; A, B, \sigma_d^2)$ in the range P_k. The goal is to find the set of parameters $\overline{A}$, $\overline{B}$, and $\overline{\sigma_d^2}$ that minimize the total squared error between the model and the histogram:

$$\left\{\overline{A}, \overline{B}, \overline{\sigma_d^2}\right\} = \arg \min_{A,B,\sigma_d^2} \left\{ \sum_{k=1}^{N} \left| h_k - \int_{\frac{(k-1)V_{max}}{N}}^{\frac{kV_{max}}{N}} P_R(r; A, B, \sigma_d^2) dr \right|^2 \right\}. \tag{14}$$

The Doppler shift is determined from the power spectral density of the envelope. The power spectral density is obtained by squaring the signal envelope voltage, Equation (5) to get

$$\begin{aligned} e^2(t) &= [A + B\cos(\theta + \Delta\omega t)]^2 + B^2 \sin^2(\theta + \Delta\omega t) \\ &= A^2 + B^2 + 2AB\cos(\theta + \Delta\omega t). \end{aligned} \tag{15}$$

The autocorrelation of the signal envelope is then computed by

$$R_{e^2}(\tau) = \lim_{T\to\infty} \frac{1}{2T} \int_{-T}^{T} e^2(t)e^2(t+\tau)dt \tag{16}$$

$$= \left(A^2 + B^2\right)^2 + 2A^2B^2\cos(\Delta\omega\tau), \tag{17}$$

and the power spectral density of the envelope squared is then the Fourier Transform of Equation (17)

$$S_{e^2}(\omega) = 2\pi\left(A^2 + B^2\right)^2 \delta(\omega) + 2\pi A^2B^2\left[\delta(\omega - \Delta\omega) + \delta(\omega + \Delta\omega)\right]. \tag{18}$$

The largest nonzero frequency component in the power spectral density gives an estimate of the relative Doppler shift $\Delta\omega$.

The minimizing set of $\bar{A}$, $\bar{B}$, and $\bar{\sigma}_d^2$ from Equation (14) results in a pdf curve that matches the histogram points from the observed signal envelope data, with the squared error as an indication how well they match. Typical parameters for the channel can be found from Equations (3) and (4). An example of the probability density function and cumulative density function for a particular data set can be seen in Figure(l).

RESULTS AND CONCLUSIONS

Typical results for various data runs can be seen in Table(l). Γ varies from 0 to 1 as expected, and κ ranges from -48 to 25 dB, with typical values between 10 and 20 dB. The Doppler shift varies from 0 Hz to 1.45 Hz. There seems to be no correlation between any of the parameters and the ability of the model to predict the parameters of the channel as evidenced by the squared error. The high values of squared error for the data from Pax River are due to assumptions in the calculation of the RF voltage envelope (see Appendix A). The narrow band channel model model presented in this paper seems to accurately model signal envelopes under varied circumstances, including both environments with a dominant line-of-sight signal component as well as environments where the power in the specular reflections is on the order of the power in the line-of-sight component.

Table 1: Power Ratios for Best Fit Parameters

Location	Data Segment	Polarization	Γ	κ (dB)	Doppler (Hz)	SQ ERR $x10^{-5}$
Edwards	1	LHCP	0.0270	13.72	0.45	12.784
Edwards	1	RHCP	0.0280	14.86	0.45	38.770
Edwards	2	LHCP	0.3541	13-13	1.37	7.051
Edwards	2	RHCP	0.1535	14.99	1.37	13.210
Edwards	3	LHCP	1.0000	11.97	1.07	15.949
Edwards	3	RHCP	0.6548	13.59	1.07	25.539
Edwards	4	LHCP	0.6591	11.56	1.45	10.615
Edwards	4	RHCP	0.5987	11.60	1.45	9.681
Edwards	5	LHCP	0.7592	9.44	1.07	35.633
Edwards	5	RHCP	0.5630	11.54	1.07	14.745
Edwards	6	LHCP	2.5E-7	16.83	0.00	12.441
Edwards	6	RHCP	64E-6	17.90	0.00	47.171
White Sands	1	LHCP	9.7E-5	24.42	0.53	56.017
White Sands	2	LHCP	1.0000	-48.2	0.00	29.999
White Sands	3	LHCP	2.3E-6	12.02	0.23	32.010
White Sands	4	LHCP	0.0112	22.21	0.27	3.3127
Pax River	1	LHCP	0.3969	9.08	0.53	140
Pax River	2	LHCP	0.1423	10.46	0.38	500
Pax River	2	RHCP	0.9818	7.64	0.38	440
Pax River	3	RHCP	0.1637	14-66	0.61	190
Pax River	4	LHCP	1.6E-9	11.32	0.92	310
Pax River	4	RHCP	0.0235	12.75	0.92	190

APPENDIX A: DATA COLLECTION AND ENVELOPE CALCULATION

Brigham Young University's Data Acquisition System (DAS) sampled Automatic Gain Control (AGC) voltages at Edwards AFB and White Sands Missile Range using a sample rate of 50,000 Hz then filtered it to 10,000 Hz, and sampled AGC voltages at Pax River NAWS using of sample rate of 20,000 Hz. The data from Edwards AFB was recorded from the telemetry of a B2 bomber in December 1995 with carrier frequency 2.225 GHz, data rate 1.2 Mbps, IF bandwidth 1.5 MHz and AGC time constants set at 1ms. The telemetry data from White Sands had carrier frequency 2.2345 GHz, data rate 352 kbps, IF bandwidth 750 kHz and AGC time constants set at 1ms. The data from Pax River was sampled from the telemetry of Super Hornet and E5 Hornet test flights over the ocean, with carrier frequency 2.3455 MHz and IF bandwidth 15 Mhz.

The AGC voltages from Edwards and White Sands were supplemented by AM envelope levels, increasing the accuracy of RF envelope reconstruction. Dye [2] and Hill [4] showed that each sample of the RF envelope can be reconstructed using the equation

$$e_s[i] \;=\; C \cdot \frac{e_a[i]}{K_2 10^{\frac{e_g[i]}{K_1}}} \tag{19}$$

where K_1 and K_2 are receiver constants, e_a and e_g are the digitized AGC and AM voltages, and C is a gain constant determined by the receiver. While this gain constant will affect absolute power levels, it will not affect power level ratios, so it need only be constant for the data used in a particular analysis run.

If the AGC voltage is assumed to track the signal level perfectly, the AM envelope is not needed in the calculation of the RF signal envelope [5]. Since the AM levels were not recorded at Pax River, this assumption was made, and the RF envelope was reconstructed according to

$$e_s[i] \;=\; C v_n 10^{\frac{SNR}{20}} \tag{20}$$

where the Signal to Noise Ratio (SNR) was calulated using a linear point-slope equation and the receiver constants. This resulted in a loss of accuracy, but some satisfactory results were still obtained.

REFERENCES

[1] P. A. Bello. Aeronautical channel characterization. *IEEE Trans. Commun*, COM-21:658-662, May 1973.

[2] Ricky G. Dye Signal Strength Analysis of Angle Modulated Data in the Presence of Multipath Fading. Master's thesis, Brigham Young University, 1996.

[3] Michael Rice and Daniel Friend. Antenna gain pattern effects on multipath interference in aeronautical telemetering. In *Proceedings of the International Telemetering Conference*, volume 33, October 1997.

[4] E. R. Hill. *Time Domain Analysis of an Automatic Gain Control Weighted Diversity Combining System, Technical Publication TP-73-47*. Naval Missile Center, Point Mugu, CA, December 1973.

[5] E. R. Hill. *Techniques and Circuits for Implementing Predetection Diversity Combiners, Technical Publication TP-78-20*. Pacific Missile Test Center, Point Mugu, CA, September 1978.

[6] B. W. Lindgren. *Statistical Decision Theory*. McMillan, New York, 1976.

[7] N. Tom Nelson. Performance analysis of PCM/FM in the presence of multipath fading. Master's thesis, Brigham Young University, 1995.

[8] Athanasios Papoulis. *Probability, Random Variables, and Stochastic Processes*. McGraw-Hill, Inc., third edition, 1991.

[9] Michael Rice and Gene Law. Aeronautical telemetry fading sources. *In Proceedings of the International Telemetering Conference*, volume 33, October 1997.

[10] Seymour Stein. Fading channel issues in system engineering. *IEEE Journ. Select. Areas Comm.*, SAC-5(2):68-89, February 1987.

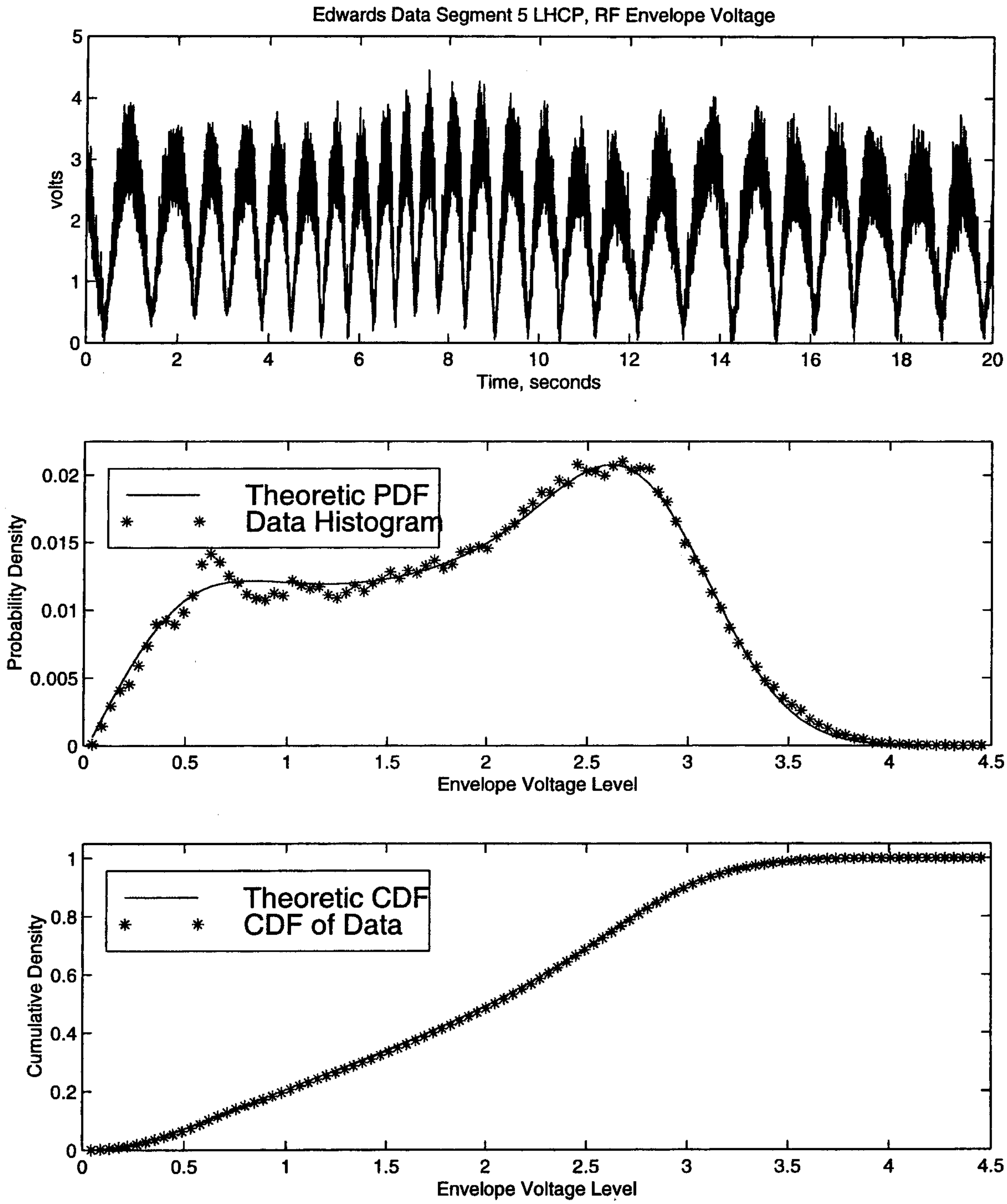

Figure 1: Envelope voltage, probability density function, histogram and cumulative density function for Edwards run 5, LHCP with Γ=0.7592 and κ=9.76 dB, with total squared error=$35.633 \cdot 10^{-5}$.